Thermochimica Acta, 18 (1977) 177–196

THERMAL AND MÖSSBAUER STUDIES OF IRON-CONTAINING HYDROUS SILICATES

I. NONTRONITE

K. J. D. MACKENZIE AND D. E. ROGERS
Chemistry Division, D.S.I.R. Private Bag, Petone (New Zealand)
(Received 20 May 1976)

ABSTRACT

DTA, TG, X-ray diffraction, infrared and Mössbauer studies of the thermal transformations of ferric and ferroan nontronites in air, argon and hydrogen/nitrogen have in all cases shown a continuity between reactant, intermediate and product phases. The nature of the intermediate and product phases is determined by the ferrous/ferric ratio of the starting material and, towards the end of dehydroxylation, by the redox potential of the reaction atmosphere. The major products can include hematite, magnetite, fayalite, ferrosilite, iron metal and a siliceous phase, the nature of which is determined by the reaction atmosphere which may control the degree of tetrahedral substitution during the reaction. Some evidence is presented for the formation of an iron–silicon spinel based on maghemite, and possible inhomogeneous reaction mechanisms are suggested on the basis of structural continuity during the reaction.

INTRODUCTION

Thermal studies of minerals provide information both about their high-temperature chemistry and, indirectly, about their room-temperature constitution. Work on the iron-containing minerals is complicated by the atmosphere-dependence of their thermal reactions and their tendency to undergo simultaneous reactions, i.e., oxidation and dehydroxylation[1]. Investigations of such minerals should, therefore, include work in oxidising, inert and reducing atmospheres. The scant attention paid previously to this aspect has led to the present studies of a number of iron-containing hydrous silicate minerals.

Mössbauer spectroscopy has proved extremely useful in investigating iron-containing minerals[2] and, in the present work, it has been used in conjunction with DTA, TG, X-ray powder diffraction and IR spectroscopy to monitor changes in the state of the iron, particularly during dehydroxylation.

Nontronites are the iron-rich members of the dioctahedral smectite series which also includes aluminous montmorillonite and beidellite. The ideal formula is $[Si_{7.34}Al_{0.66}]Fe_4^{3+}O_{20}(OH)_4 \cdot nH_2O(\frac{1}{2}Ca, Na)_{0.66}$. In natural nontronites, there is

usually some substitution of magnesium for iron in the octahedral sites (Table 1). In ferroan nontronites, which contain a higher proportion of ferrous ions (probably in octahedral sites[3]), substitution of ferric iron for aluminium also occurs in the tetrahedral sites (Table 1). Thus, ferroan nontronite is intermediate between ferric nontronite and a presently unknown ferrous iron end member.

Although nontronite has been studied more fully than any of the other minerals included in the present series of experiments, it was re-investigated here because of its possible relationship with some of the other minerals to be studied (i.e., hisingerite[4]). In addition, such thermal studies of nontronite as have been reported[5,6] are not in complete agreement. Thus, Grim and Kulbicki[5] found that both dehydroxylation and the destruction of the smectite lattice occur at lower temperatures than in aluminous smectites. The loss of structure was gradual, and not accompanied by a DTA peak; again, an exotherm between 800–900°C was not accompanied by the appearance of any crystalline phase detectable by X-ray diffraction. The only high-temperature crystalline phase reported was β-cristobalite, which appeared at about 1200°C; the absence of any other crystalline phases was attributed to retardation caused by the presence of iron[5]. By contrast, Bradley and Grim[6] reported the development at about 1300°C of mullite, cristobalite and an (iron-containing?) spinel from a nontronite having an identical DTA trace to that studied by Grim and Kulbicki[5]. The effect of the reaction atmosphere, particularly on dehydroxylation, was not taken into account in either of these studies.

Mössbauer spectra have been published for unheated ferric nontronites[7,8] and a ferroan nontronite[3], but no Mössbauer studies of the intermediates in the thermal reactions have been reported.

EXPERIMENTAL

(*a*) *Materials*

One of the nontronites studied was a well-characterised ferric mineral from Washington State, U.S.A., obtained from the N.Z. Geological Survey collection (No. 39184). This was a fine-grained yellow material having the characteristic X-ray pattern (A.S.T.M. 13-508) with an interlayer spacing of 15.6 Å. The chemical analysis of this material is given in Table 1, and the resulting structural formula, calculated by the method of Ross and Hendricks[9] is given in Table 2, column 2. Scanning electron micrographs of this material show a typical platy texture.

The ferroan nontronite was a dark olive-green material from the Penge area of Eastern Transvaal, and is a subsurface weathering product of an amosite asbestos deposit and associated banded iron-stone rocks. The X-ray pattern showed the principal nontronite lines, with an interlayer spacing of 15.4 Å. Small traces (<5%) of quartz and goethite were detectable by X-ray diffractometry. The chemical analysis (Table 1) and structural formula (Table 2) show this mineral to be very similar to the ferroan nontronite described by Bischoff[3] (Table 2, column 5), although the genesis of the two minerals is dissimilar. Scanning electron micrographs again

TABLE 1

ANALYSES OF NONTRONITES

Major element analysis by atomic absorption trace element analyses by semi-quantitative arc spectroscopy.

Element	*Ferric* (%)	*Ferroan* (%)	*Element*	*Ferric* (*ppm*)	*Ferroan* (*ppm*)
SiO_2	38.76	33.53	Cr	100	20
Al_2O_3	5.45	2.16	Cu	50	50
Fe_2O_3	29.25	40.07	Ni	25	25
FeO	0.15	3.59	V	50	25
MgO	0.67	1.89	Zn	25	25
CaO	1.55	0.71	Pb	25	1
Na_2O	0.17	0.33	Ag	10	100
K_2O	—	1.49	Ga	5	5
H_2O	18.86	16.00	Ge	—	5
SO_3	5.00	—	Sr	100	—
MnO	0.03	0.02			
TiO_2	0.21	0.14			
Total	100.10	99.93			

TABLE 2

FORMULAE OF NONTRONITES

		1	*2*	*3*	*4*	*5*
Si	tet.	7.34	6.86	7.34	5.98	6.29
Al	tet.	0.66	1.14	0.66	0.42	0.52
Fe^{III}	tet.	—	—	—	1.60	1.19
Fe^{III}	oct.	4.0	3.90	3.60	3.74	3.19
Fe^{II}	oct.	—	0.02	—	0.54	0.49
Mg	oct.	—	0.32	0.50	0.54	0.37
½Ca	exch.	0.66	0.53	—	0.22	0.20
Na	exch.		0.05	—	0.10	1.10
K	exch.	—	—	—	0.32	0.18

Column 1. Ideal formula.
Column 2. Ferric nontronite, this study. Analysts R. Goguel and J. Ritchie.
Column 3. Type mineral (Nontron). Analysis from ref. 9.
Column 4. Ferroan nontronite, this study. Analysts R. Goguel and J. Ritchie. Allowance made for quartz impurity.
Column 5. Ferroan nontronite, Bischoff, sample 128P, from ref. 3.

show a platy texture; in some areas fibres of a possible amphibole contaminant could also be seen.

(*b*) *Techniques*

DTA studies were made under air, argon and forming gas (5%H_2/95%N_2) in

a Stone Model 202 thermal analyser at a heating rate of 10°C min^{-1}. Samples for further examination were heated for 0.5 h in the various atmospheres to temperatures selected by reference to the DTA traces, and maintained under the reaction atmosphere during cooling. TG curves were obtained on a Chevenard thermobalance in ambient air at a heating rate of 2.5°C min^{-1}.

The fired samples were examined using Cu-X-radiation in a Philips diffractometer equipped with a graphite monochromator which eliminated the effect of sample fluorescence. IR spectra were obtained on Beckman IR 12 and Perkin-Elmer 337 spectrophotometers using samples suspended in KBr discs. The Mössbauer spectra were obtained from a linear velocity drive spectrometer based on a design by Clark et al.[10] using a Co/Pd source. The spectra were computer fitted to Lorentzian lineshapes by a programme based on that of Stone et al.[11], from which all the parameters were obtained. Isomer shifts were measured relative to soft iron.

RESULTS AND DISCUSSION

(*a*) *Thermal analyses*

The DTA traces of the two nontronites in the various atmospheres are shown in Fig. 1. These traces are broadly similar to those previously published[5,6], showing endothermic dehydration and dehydroxylation at 100–600°C, and various higher temperature peaks related to the crystallization of the anhydrous phases. Figure 1 shows that the interlayer water is lost in several stages, which are also reflected as plateaux in the TG curves, particularly in the ferroan sample. The first water loss from this sample, corresponding to a 10.7% weight loss, is complete by about 150°C, while the next weight loss (1.3%) is complete by about 300°C in air. The occurrence of this process in at least two stages may be related to the presence of iron in the various sites adjacent to the water molecules, since these DTA peaks are further split in the ferroan sample under reducing conditions which should prevent the ferrous ions from oxidising during water loss. The total weight losses below 300°C correspond to the loss of 6 and 7.5 moles of interlayer water from the ferroan and ferric nontronites, respectively, but this figure may be slightly high because of overlap with the onset of dehydroxylation. The dehydroxylation endotherm is accompanied in ferroan nontronite by a rapid 1.8% weight loss up to 400°C, followed by a more gradual loss of a further 1.8% ending at about 700°C. The theoretical dehydroxylation weight loss, calculated from the chemical analysis of the ferroan sample is 3.96% of the sample weight after loss of interlayer water. On the same basis, the total weight loss observed during dehydroxylation is 4.08%, in good agreement with the calculated value. The corresponding weight-loss values for ferric nontronite are not in good agreement (4.49% calculated, 5.38% observed), probably due to overlap of dehydration and dehydroxylation. The calculations suggest that both weight losses in ferroan nontronite above about 350°C are associated with dehydroxylation, which proceeds in an initially rapid manner but tails off in the later stages. A similar but less marked tailing-off of weight loss occurs at higher temperatures during kaolinite dehydroxyla-

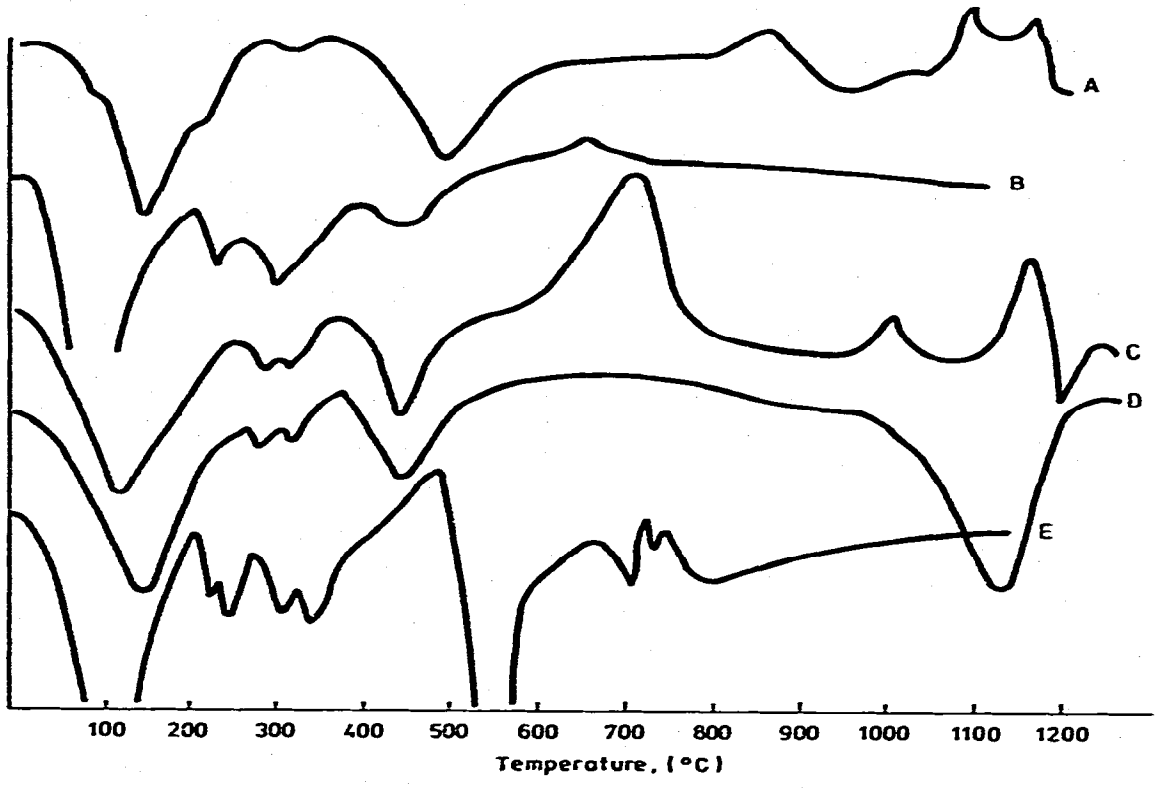

Fig. 1. DTA traces of nontronites, heating rate 10°C/min^{-1}. (A) Ferric nontronite in air or argon. (B) Ferric nontronite in H_2/N_2. (C) Ferroan nontronite in air. (D) Ferroan nontronite in argon. (E) Ferroan nontronite in H_2/N_2.

tion, and is characteristic of a material in which a proton-stabilized dehydroxylate is formed which slowly recrystallizes at higher temperatures[12]; it seems reasonable that iron and aluminium silicates should have similar proton retention properties.

At temperatures above dehydroxylation, the DTA traces reveal differences in behaviour between the two nontronites under the various atmospheres. The traces for ferric nontronite are identical under air and argon (Fig. 1), but in H_2/N_2 the dehydroxylation endotherm and subsequent crystallization exotherm are lowered in temperature by about 50 and 200°C, respectively. Differences in the DTA traces of ferroan nontronite are even more marked; three exotherms recorded in air are replaced by a single, high-temperature endotherm in argon, while in H_2/N_2, a complex endotherm–exotherm appears at about 700°C.

Since the two nontronites differ principally in their concentration of ferrous ions, the large exotherm in the ferroan sample in air at about 700°C was shown by Mōssbauer spectroscopy (Section d) to be associated with the oxidation of Fe^{2+} to Fe^{3+}, followed by the crystallization of hematite (α-Fe_2O_3). The broadness of this peak, which starts at about 520°C suggests a progressive rather than a sharp reaction. This oxidation is suppressed in argon, in which the principal product of initial crystallization should be magnetite, Fe_3O_4. Since the argon used in this work had a

small but significant oxygen content, some hematite will be expected at higher temperatures; the endotherm at 1130°C of ferroan nontronite in argon could be explained by the oxidation of the magnetite to hematite. According to the oxygen potential diagram of Richardson and Jeffes[13], this oxidation is endothermic by about 104.5 kJ mol^{-1} at 1100°C, and would proceed at this temperature at an oxygen partial pressure of about 10 Pa (10^{-4} atm). This compares quite well with the manufacturer's value for the oxygen content of the argon used here (<10 ppm by volume). At still higher temperatures, above the range of the present DTA traces, the stability of magnetite increases, and this should become the sole iron-containing phase present.

(b) X-ray diffraction

The phases formed from the two nontronites under oxidising, inert and reducing atmospheres are shown schematically as a function of temperature in Fig. 2. The first reaction detectable by X-ray diffraction is the loss of interlayer water, resulting in a collapse of the interlayer spacing from 15.5 to 9.6 Å and 10.0 Å in the ferric and ferroan samples, respectively (the nature of the cations trapped in the intersilicate positions after the loss of the water with which they were associated largely determines this spacing[14], which is independent of the reaction atmosphere). Although the 10 Å structure persists up to temperatures at which some hydroxyl water is lost, we prefer to term this phase a dehydrate rather than a dehydroxylate, since, apart from the interlayer spacing, the X-ray pattern is identical to the original material.

Molloy and Kerr[14] have reported that a peak at about 3.16 Å develops after heat treatment at 550°C, and suggest that this peak is diagnostic for the dehydrated phase. We observe a peak in this region in our unheated samples (all the nontronite peaks are rather broad), which suggests that Molloy and Kerr's diagnostic peak is a characteristic of the parent material. In their sample, this peak may have been of low intensity but became more apparent after heating; a slight intensification and shift of this peak to lower angle was noted in some of our samples after heating.

Figure 2 shows that the temperature of both formation and decomposition of the dehydrate phase is lowered by reducing atmospheres in both nontronites, but in addition, ferric nontronite at lower temperatures develops a transitory phase with an X-ray pattern resembling fayalite, Fe_2SiO_4.

On heating to higher temperatures, complete dehydroxylation is indicated by the loss of the dehydrate peaks. The destruction of the nontronite structure is concomitant with the appearance of product phases. Under inert or oxidising conditions, the discrete oxides of iron and silicon are formed, but under reducing conditions, the presence of predominantly Fe^{2+} favours the initial formation of ferrous silicates rather than the oxides, with the excess iron or silicon appearing later as iron metal or wustite (FeO) and quartz, respectively. In oxidising and neutral conditions, the formation of hematite is preceded by maghemite (γ-Fe_2O_3). This phase has a defect spinel structure whose most intense X-ray reflection is close to the major reflection

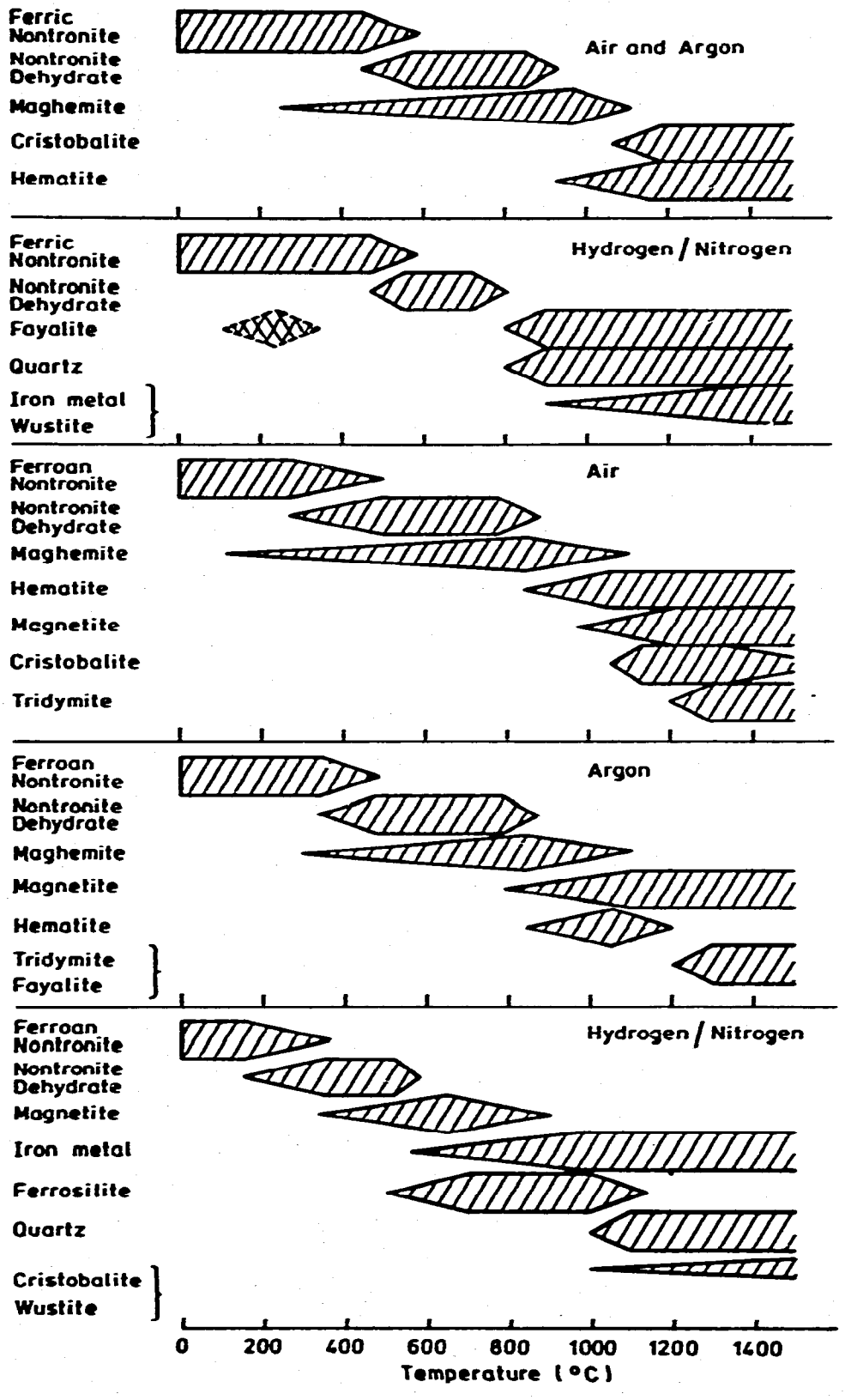

Fig. 2. Schematic diagram of the phases formed from nontronites as a function of temperature under oxidising, inert and reducing atmospheres.

of the ferroso–ferric spinel Fe_3O_4. The two are, however, distinguishable by the presence of additional superlattice reflections in the former. The precise nature of the iron-containing phases depends on the ferrous/ferric ratio of the material, which in turn depends on the starting material and the reaction atmosphere. Ferric nontronite in air or argon forms only hematite, whereas ferroan nontronite in air forms a mixture of hematite and magnetite. In argon, oxidation of Fe^{2+} in the ferroan sample is suppressed, and magnetite is the sole phase. In reducing conditions, reduction of Fe^{3+} in ferric nontronite apparently occurs before the complete destruction of the dehydrate. The resulting ferrous silicate (fayalite) which occurs without the formation of crystalline intermediates, is accompanied later by the products of further reduction (iron metal and wustite). By contrast, under reducing conditions the Fe^{2+} component of ferroan nontronite forms some magnetite even before dehydroxylation is complete; this phase is further reduced to iron metal at higher temperatures. The resulting depletion of Fe^{2+} leads to the formation of ferrosilite ($FeSiO_3$) rather than the less siliceous fayalite. The X-ray pattern of the ferrosilite corresponds to the monoclinic form (A.S.T.M 17-548); the formation of this phase in the present system is unusual since it is normally formed only at elevated pressures[15]. At higher temperatures this phase is further reduced to quartz and α-iron, the latter undergoing a progressive transformation to the austenite structure at about 1100°C.

In both nontronites, the nature of the siliceous phase depends on the reaction atmosphere, quartz being formed under reducing conditions and cristobalite or tridymite under oxidising or inert conditions. In ferroan nontronite, tridymite is the preferred final phase, probably due to the presence of a comparatively high concentration of potassium in this nontronite, which stabilises the tridymite structure[16].

(*c*) *Infrared spectroscopy*

The IR spectra of both nontronites heated in the various atmospheres are very similar, and typical spectra are shown in Fig. 3. The spectra of both unheated nontronites correspond to that of ferric nontronite published by Farmer and Russell[17], and the present interpretation of changes in the spectra of the heated materials is based on the assignments of these authors.

The loss of interlayer water does not initially affect the spectra, but with increasing water loss, the intensity of the group of peaks at 775–815 cm^{-1} decreases, as does the shoulder at about 600 cm^{-1}. The latter is assigned by Farmer and Russell to an R^{3+}–OH vibration. The former peaks which were previously unassigned are probably also associated with metal–OH vibrations, since they are the first to be affected by dehydration, which also involves the loss of some hydroxyl water, as shown by an intensity decrease in the hydroxyl stretching band at about 3600 cm^{-1}. Progressive dehydroxylation is accompanied by broadening and loss of detail from the spectra and the loss of the hydroxyl band, which occurs at about 150 degrees lower in reducing atmospheres than in oxidising or inert atmospheres.

The peak at about 845 cm^{-1} was assigned by Farmer and Russell[17] to an Fe^{3+}–OH bending mode because this peak was diminished by reduction with

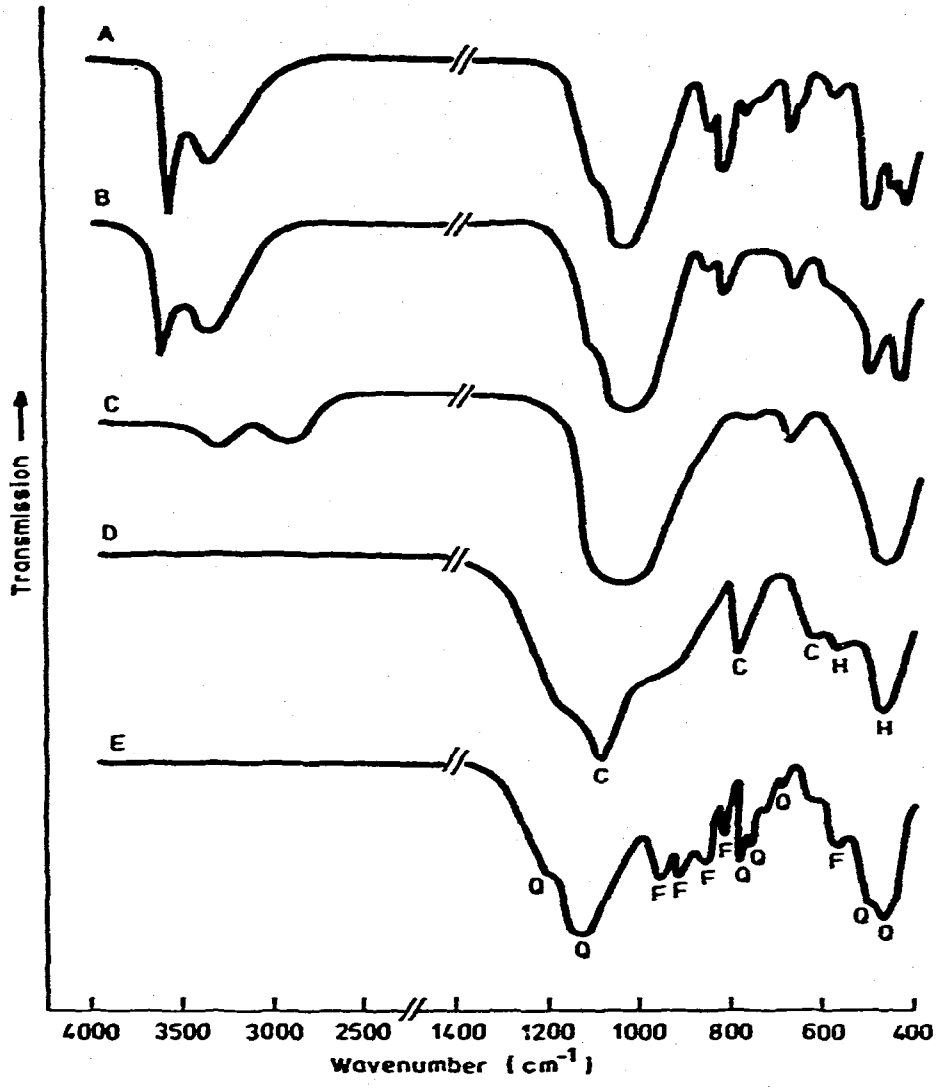

Fig. 3. Infrared spectra of heated nontronites. (A) Unheated. (B) 360°C in air or argon. (C) 580°C in air or argon. (D) 1280°C in air or argon. (E) 1100°C in H_2/N_2. H = hematite; C = cristobalite; Q = quartz; F = fayalite.

hydrazine. The present reduction experiments do not support this assignment; this peak was unaffected by hydrogen reduction and like its companion at 820 cm^{-1} decreased in intensity equally on dehydroxylation.

After dehydroxylation, only three broad peaks remain (Fig. 3, curve C). The peaks at about 1050 and 680 cm^{-1} are associated with Si–O vibrations, while the peak at about 450 cm^{-1} is an Fe–O (or R^{3+}–O–Si) vibration. In ferroan nontronite, an Si–O peak occurs at about 800 cm^{-1} after dehydroxylation; this peak develops in ferric nontronite only at a later stage in the heating. Spectral differences in the region 680–800 cm^{-1} are probably associated with vibrations of Fe^{2+}-containing species,

since considerable structure occurs in this region in samples dehydroxylated in hydrogen.

At higher temperatures, the spectra sharpen and new peaks develop, according to the product phases present. In ferroan nontronite, the first new peak to occur is an R–O peak at 550 cm^{-1}, followed by a peak at 670 cm^{-1}, probably an Si–O vibration (Fig. 3, curve D). In ferric nontronite, the 800 cm^{-1} peak develops at this stage, and the peak at 670 cm^{-1} characteristic of the dehydroxylate shifts to about 600 cm^{-1}, eventually becoming a doublet composed of an Si–O and Fe–O vibration. The spectra of samples heated in air and argon (Fig. 3, curve D) eventually resemble the spectrum

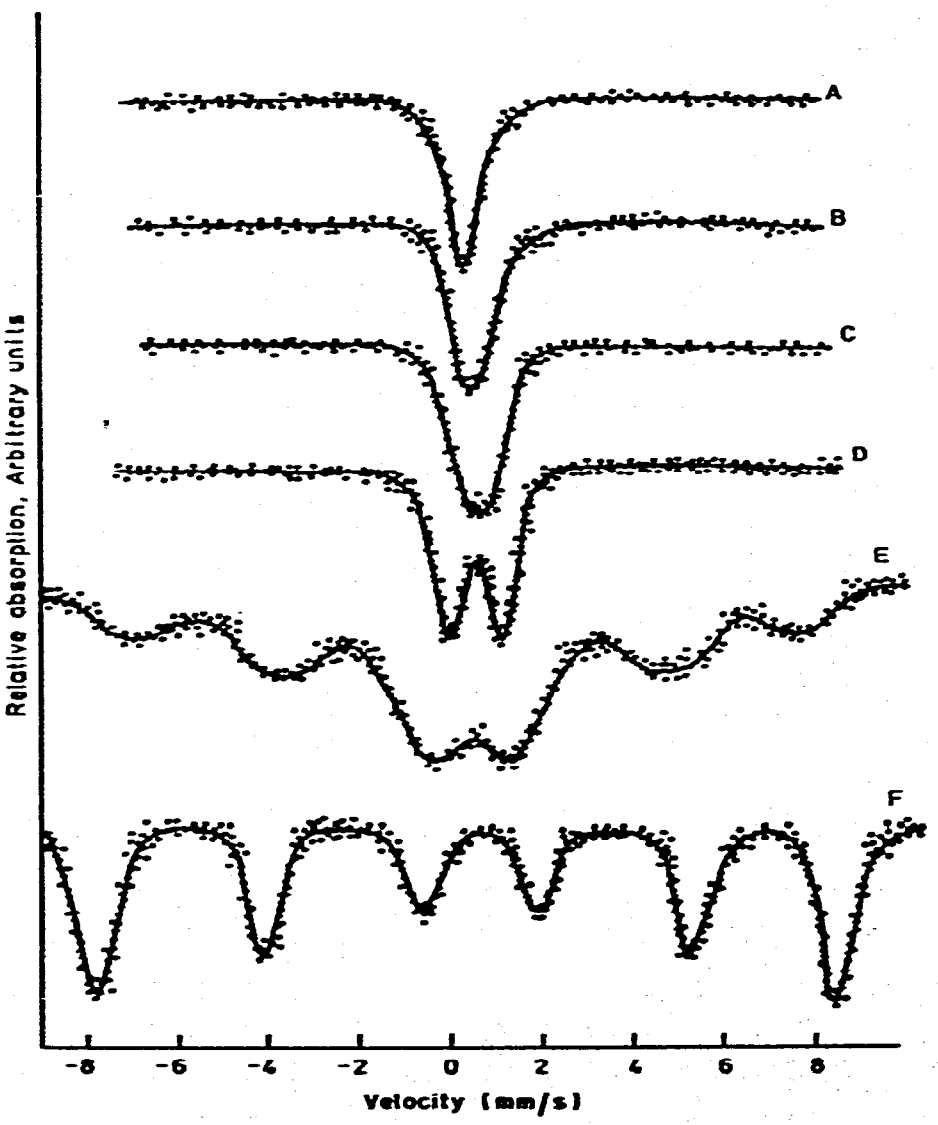

Fig. 4. Mössbauer spectra of ferric nontronite heated in argon. (A) Unheated. (B) 280°C. (C) 360°C. (D) 580°C. (E) 940°C. (F) 1280°C.

of a mixture of hematite (or magnetite) and cristobalite (or tridymite) while the spectra of samples heated in hydrogen (Fig. 3, curve E) are similar to that of a mixture of fayalite[18] and quartz[19]. Although ferroan and ferric nontronite produce ferrosilite and fayalite, respectively, their IR spectra are similar. Even after the decomposition of ferrosilite to quartz and iron metal, the retention of the spectrum suggests that at least some of the atoms are retained in an environment similar to that of ferrosilite, even though this phase has become undetectable by X-ray diffraction.

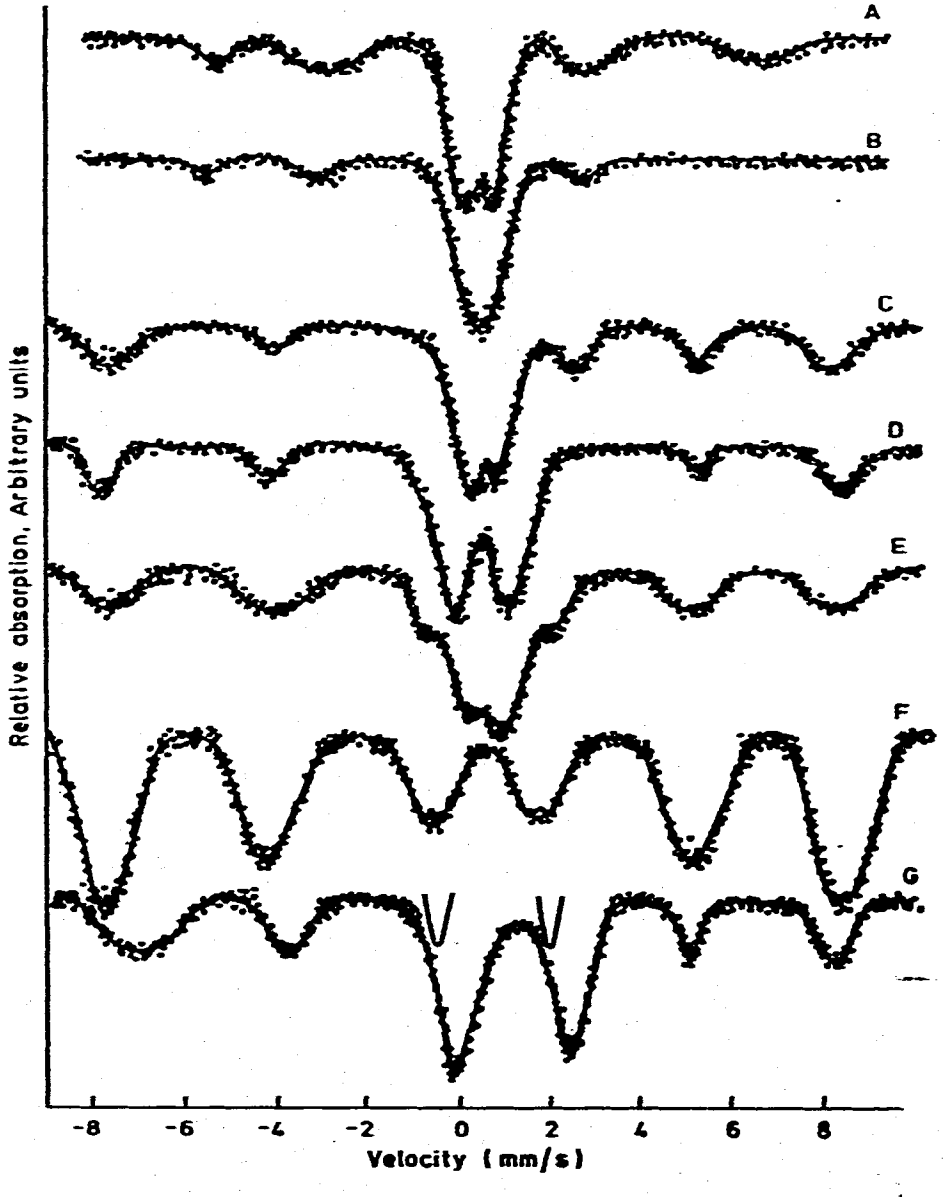

Fig. 5. Mössbauer spectra of ferric nontronite heated in H_2/N_2. (A) Unheated. (B) 150°C. (C) 240°C. (D) 320°C. (E) 560°C. (F) 1100°C.

The overall trends of the IR spectra, therefore, suggest that the reactions do not involve a sudden lattice disruption, but are more characteristic of progressive atomic rearrangements.

(*d*) *Mössbauer spectroscopy*

Typical Mössbauer spectra of ferric and ferroan nontronites heated in argon and H_2/N_2 are shown in Figs. 4–7. The Mössbauer parameters are collected in

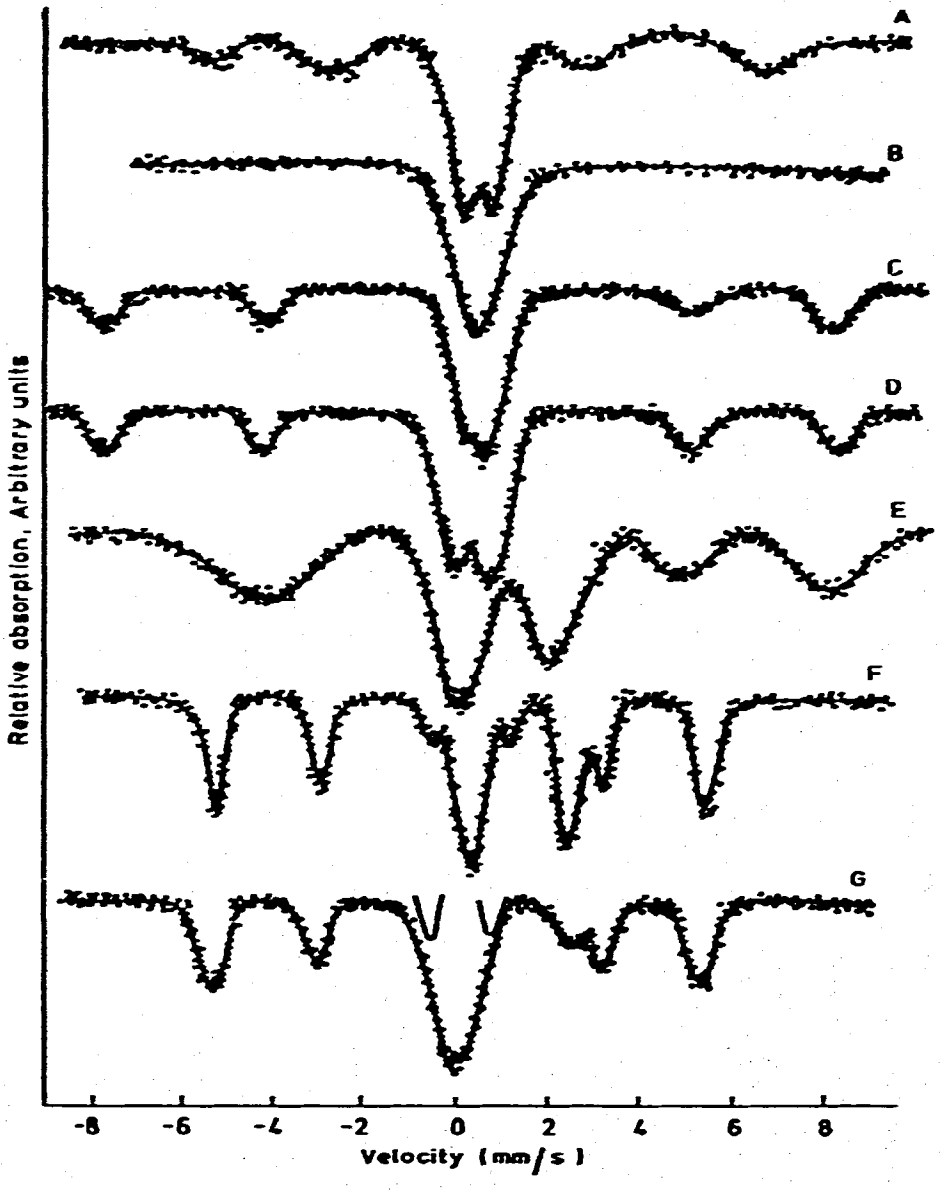

Fig. 6. Mössbauer spectra of ferroan nontronite heated in argon. (A) Unheated. (B) 175°C. (C) 340°C. (D) 500°C. (E) 840°C. (F) 1100°C. (G) 1325°C.

Table 3. The spectra of samples heated in air are similar to those reacted in argon except at the highest temperatures, where characteristic hematite spectra were recorded for all samples heated in air.

The spectrum of unheated ferric nontronite is identical to those previously published, with a single peak, thought to be an unresolved doublet[7,8] having an isomer shift characteristic of octahedral high-spin Fe^{3+}. During the removal of interlayer water, this peak broadens and its isomer shift becomes more positive until

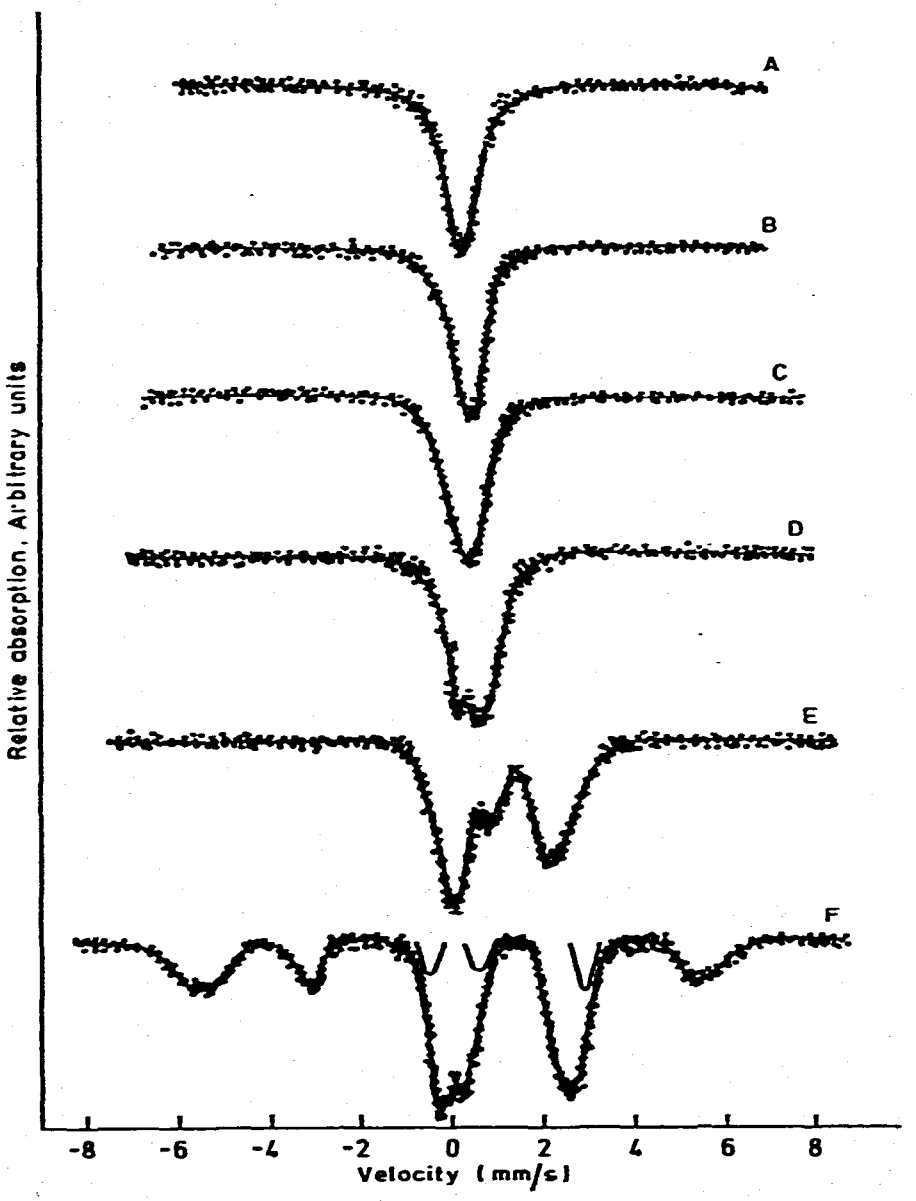

Fig. 7. Mössbauer spectra of ferroan nontronite heated in H_2/N_2. (A) Unheated. (B) 150°C. (C) 250°C. (D) 360°C. (E) 560°C. (F) 950°C. (G) 1100°C.

TABLE 3

MÖSSBAUER PARAMETERS FOR HEATED NONTRONITES (Six line spectra omitted)

Sample	*Heating atmosphere*	*Heating temp.* (°C)	*Isomer shift** (*mm sec*$^{-1}$)	*Quadrupole splitting* (*mm sec*$^{-1}$)	*Width* (*mm sec*$^{-1}$)	*Assignment*
Ferric nontronite	—	unheated	0.33	—	0.90	Fe^{3+} oct
Ferric nontronite	argon	280	0.54	—	1.20	Fe^{3+} oct
Ferric nontronite	argon	360	0.52	—	1.35	Fe^{3+} oct
Ferric nontronite	argon	580	0.53	1.19	0.94	Fe^{3+} oct
Ferric nontronite	H_2/N_2	150	0.52	—	0.98	Fe^{3+} oct
Ferric nontronite	H_2/N_2	240	0.46	—	1.08	Fe^{3+} oct
Ferric nontronite	H_2/N_2	320	0.44	0.46	0.80	Fe^{3+} oct
Ferric nontronite	H_2/N_2	560	0.40	0.80	0.97	Fe^{3+} oct
			1.13	2.26	1.60	Fe^{2+} distorted oct
Ferric nontronite	H_2/N_2	1100	1.18	2.83	0.79	Fe^{2+} oct
			1.41	2.38	0.78	Fe^{2+} oct
Ferroan nontronite	—	unheated	0.46	0.53	0.87	Fe^{3+} oct (+Fe^{3+} tet?)
			1.34	2.28	0.86	Fe^{2+} oct
Ferroan nontronite	argon	175	0.50	—	1.00	Fe^{3+} oct
			1.53	2.05	1.20	Fe^{2+} oct
Ferroan nontronite	argon	340	0.55	0.40	0.72	Fe^{3+} oct
			1.45	2.20	1.00	Fe^{2+} oct
Ferroan nontronite	argon	500	0.54	1.22	1.00	Fe^{3+} distorted oct
Ferroan nontronite	argon	840	0.55	0.70	1.20	Fe^{3+} distorted oct
Ferroan nontronite	H_2/N_2	150	0.52	—	1.20	Fe^{3+} oct
Ferroan nontronite	H_2/N_2	250	0.50	0.40	0.80	Fe^{3+} oct
Ferroan nontronite	H_2/N_2	360	0.38	0.68	0.82	Fe^{3+} oct
Ferroan nontronite	H_2/N_2	560	1.14	2.06	1.40	Fe^{2+} distorted oct
Ferroan nontronite	H_2/N_2	950	0.92	2.28	0.75	Fe^{2+} oct M_2 pyroxene site?
Ferroan nontronite	H_2/N_2	1100	1.34	2.52	1.00	Fe^{2+} oct M_1+M_2 pyroxene sites

*Relative to metallic iron.

it is resolved at 580°C into a broad doublet. The increase in quadrupole splitting indicated by the behaviour of this peak is characteristic of increasing distortion from octahedral symmetry in the 6-coordinated ferric site[20]. Since octahedral distortion is more likely to accompany dehydroxylation than the loss of interlayer water, the Mössbauer spectra suggest that the two processes overlap at a lower temperature than might be expected from DTA. The very broad 6-line spectrum which appears at 940°C is similar to the spectrum of hematite of very small particle size[21]; at higher temperatures the growth of these particles results in the more usual hematite spectrum.

In H_2/N_2, the lower-temperature spectra of ferric nontronite are similar to the spectra of samples in air and argon, with no reduction to Fe^{2+} detectable below 320°C. The first indication of a ferrous doublet occurs at 560°C, the parameters of which are typical of Fe^{2+} in a very distorted octahedral site[21]. This suggests that significant reduction does not occur until dehydroxylation is almost complete, and further that the transient phase observed at about 200°C having some of the X-ray characteristics of fayalite does not contain sufficient high-spin Fe^{2+} to be observed by Mössbauer spectroscopy. The possible occurrence of low-spin Fe^{II} is however, not ruled out, since this would give rise to a peak or peaks in the vicinity of the Fe^{3+} peaks, and may account for one component of the doublet observed at 320°C. The spectra of samples heated at 1100°C consist of the 6-line spectrum of metallic iron superimposed upon two more intense peaks, one of which is partially resolved into a doublet. The parameters of these peaks are typical of fayalite[22], the spectrum of which consists of two superimposed doublets which are not always resolved.

The spectrum of unheated ferroan nontronite is similar to that previously reported for a similar material[3], which has been interpreted as a combination of peaks for octahedral Fe^{3+} (at -0.2 and $+1.0$ mm sec^{-1}), tetrahedral Fe^{3+} (-0.35 and $+0.45$ mm sec^{-1}) and octahedral Fe^{2+} (-0.05 and $+2.35$ mm sec^{-1}). As in the previously reported mineral[3], the present spectrum is broad and not completely resolved. In addition, the present sample contains a weak, broad 6-line spectrum arising from the goethite impurity. Heating in argon (and in air) causes an initial loss of resolution (Fig. 6), which is re-established by 340°C, at which temperature the Fe^{2+} component is still apparent. The geothite spectrum, which was virtually destroyed by low-temperature heating, is now replaced by a wider-spaced 6-line spectrum corresponding to the maghemite-type phase[21] observed by X-ray diffraction. At higher temperatures, this spectrum develops at the expense of the inner ferric doublet, eventually becoming a characteristic hematite spectrum.

In H_2/N_2, both the goethite spectrum and the ferrous peak of ferroan nontronite have been lost by 150°C (Fig. 7). By 250°C a weak, broad 6-line spectrum has re-appeared; the X-ray data suggest that this is due to magnetite. Thus, the loss of the Fe^{2+} spectrum in the early stages of heating may be due either to the incorporation of this species into a magnetite-like phase of extremely small particle size (or micro-regions of this phase), or to the initial oxidation of Fe^{2+} as a side reaction to water loss:

$$Fe^{2+} + H_2O \rightarrow Fe^{3+} + OH^- + \tfrac{1}{2}H_2 \qquad (1)$$

Since the octahedral ferrous spectrum re-appears after further heating, the first explanation seems more likely. Further reduction causes the splitting of the Fe^{3+} peak, with an increase in its quadrupole splitting due to an increasingly distorted octahedral environment, and the re-appearance at 560°C of a broad, octahedral Fe^{2+} doublet. Further reduction of the magnetite phase causes its spectrum to become diffuse, eventually re-appearing as a 6-line metallic iron spectrum. The broadness of the Fe^{2+} doublet can be ascribed to the distortion of the octahedral sites, which eventually become the M_1 and M_2 sites of the pyroxene ferrosilite. The isomer shift and quadrupole splitting of the ferrous doublet observed after firing at 1100°C correspond most closely with the M_1 site of ferrosilite[23] but the width of these peaks suggests that they are composed of unresolved doublets corresponding to the occupancy of both sites.

In summary, the Mössbauer spectra show:

(i) Significant reduction and oxidation become apparent only towards the end of the dehydroxylation process.

(ii) The formation sequence of iron-containing phases is continuous, and dictated at lower temperatures by the initial distribution and valency of the iron atoms. At higher temperatures, significant oxidation or reduction modifies the product phases, again by a continuous process.

(iii) The Mössbauer spectra are in agreement with the phase compositions deduced by X-ray diffraction.

(*e*) *Mechanism of the thermal reactions in nontronite*

The present results show that a continuity exists between the starting material and all the subsequent phases. This result is completely different from that of a previous study[5] which suggested that although the smectite structure disappears at about 850°C, the only detectable crystalline product (cristobalite) does not appear until about 1200°C. Neither iron-containing phases nor mullite were detected in that study[5], but the suggested explanation that iron "blocks" the formation of mullite is at variance with the formation of mullite from kaolinite containing high concentrations of iron, and the fact that appreciable iron can enter into solid solution with mullite. The absence of mullite in the present samples is more likely due to the low aluminium content. The failure of Grim and Kulbicki[5] to observe intermediate phases was probably due to the poorer detection and resolution of the equipment available when their X-ray studies were made.

Structural continuity between initial, intermediate and final phases is commonly an indication of an inhomogeneous reaction mechanism involving a counter-migration of protons to "donor regions" from which water is lost, and other cations to "acceptor regions" which give rise to the product phase[12]. With the exception of a study of cronstedtite[24], previously reported work on iron-containing layer silicates gave little indication as to whether these should dehydroxylate by an inhomogeneous mechanism (as do most magnesium silicates), or by a homogeneous mechanism such as is commonly postulated for aluminium silicates[12]. The study of cronstedtite[24]

showed a structural continuity in the dehydroxylation products which has been interpreted[25] in terms of an inhomogeneous mechanism. In that case, the initial product was a spinel-resembling maghemite, but possibly containing tetrahedral silicon. The structure of this spinel is therefore similar to the Al–Si spinel postulated as an intermediate in the kaolinite–mullite reaction[26], and as in the kaolinite reaction, no free silica was detected from cronstedtite until the decomposition of this spinel to hematite[24]. The composition of a maghemite spinel with full tetrahedral substitution would be $Si_8[Fe_{10\ 2/3}\square_{5\ 1/3}]O_{32}$, but, as in the case of the analogous aluminosilicate spinel from kaolinite, some degree of proton stabilisation might also occur[27], giving a composition of $Si_8[Fe_yH_x\square_z]O_{32}$ where $y=(32-x)/3$, $z=16-(x+y)$ and $\square$ is a cation vacancy. The limiting composition of such a spinel would be $Si_8Fe_8H_8O_{32}$.

By analogy with the cronstedtite decomposition mechanism, the reaction sequence of nontronite could be interpreted in terms of an inhomogeneous mechanism, if the substitution of Si for tetrahedral Fe in the maghemite spinel is accepted. This phase has the characteristic light brown colour of maghemite, but it is considerably more stable, persisting to much higher temperatures than the simple spinel. Similar stability observed in the spinel formed from cronstedtite has been attributed to the incorporation of silicon in that phase. Schematic diagrams of possible inhomogeneous reaction mechanisms in nontronites are shown in Fig. 8. Although the structural contunuity of the sequences suggests such a mechanism, unequivocal proof would be furnished only if precise orientational relationships could be established between reactant and products. The present powder studies do not provide such information and the poor crystallinity of the samples militates against single crystal studies. Nevertheless, the reaction schemes of Fig. 8 provide a consistent explanation for all the present facts.

The formation of quartz rather than cristobalite or tridymite under reducing conditions requires comment. Observations on a number of montmorillonites[28] have shown that in materials with significant substitution of tetrahedral silicon, the transformation product is a spinel, the siliceous phase appearing at higher temperatures as cristobalite. In materials having little tetrahedral substitution, the initial siliceous product is quartz, which transforms to cristobalite only at higher temperatures. On this basis, the formation of quartz in nontronites under reducing conditions suggests that foreign ion substitution in the tetrahedral layers is decreased by reduction. In ferroan nontronite, tetrahedral Fe^{3+} is reduced to Fe^{2+}, which ion has an octahedral site preference energy of about -4 kJ mol^{-1}, compared with Fe^{3+}, which has a *tetrahedral* site preference energy of about -16 kJ mol^{-1} (ref. 29). Thus, reduction of tetrahedral Fe^{3+} should result in a tendency for the iron to move to octahedral sites, facilitating the separation of quartz from the siliceous regions. This reasoning is not so easily extended to ferric nontronite, in which the formation of quartz under reducing conditions could mean either that contrary to the accepted structure, appreciable tetrahedral substitution of ferric iron occurs (this is not supported by Mössbauer evidence) or that the reduction of the octahedral Fe^{3+} leads to a charge imbalance which is compensated for by migration of aluminium

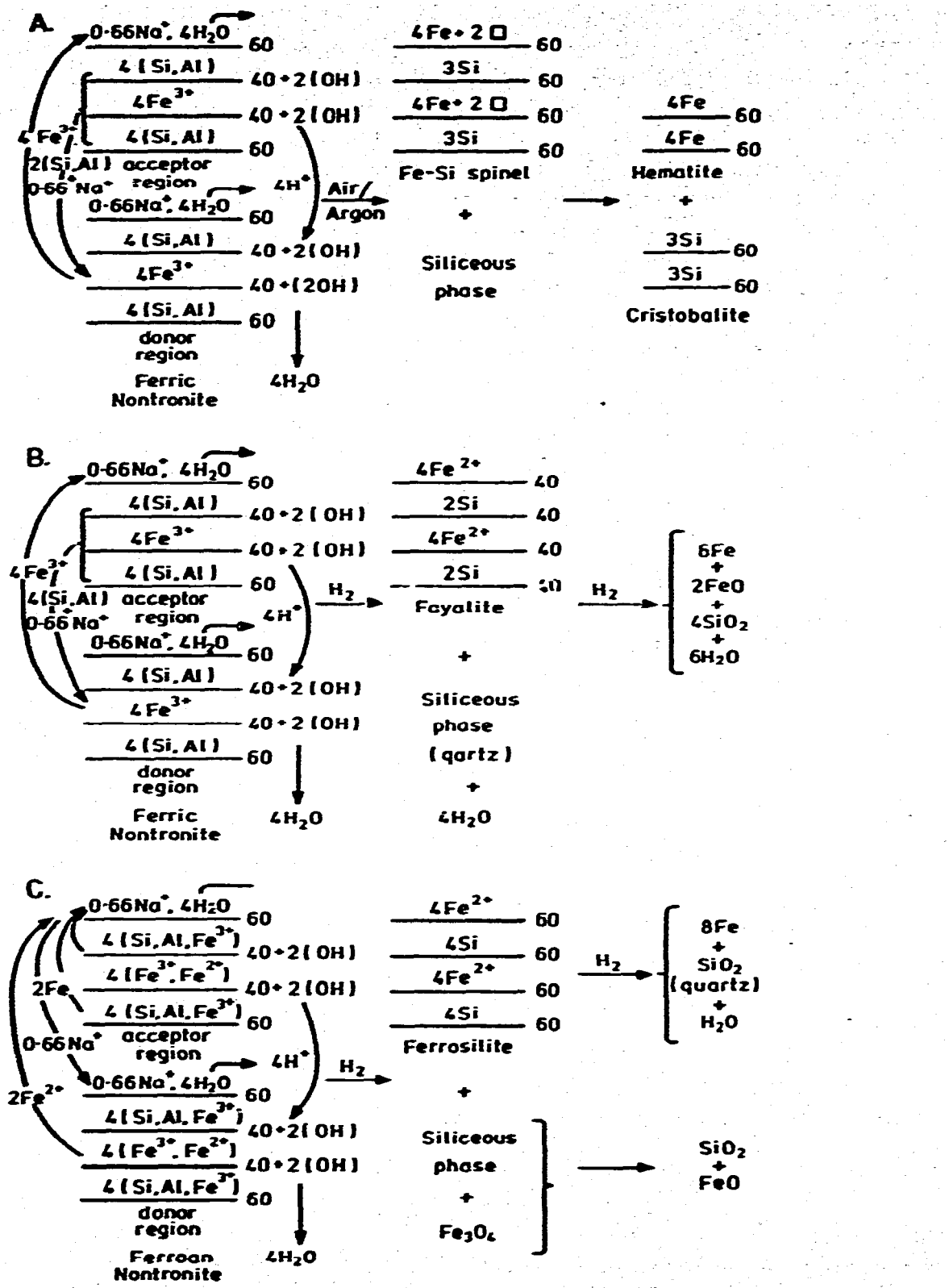

Fig. 8. Schematic diagram of possible inhomogeneous mechanism for thermal transformations of nontronites. Horizontal lines represent oxygen layers in approximately close packing. (A) Ferric (or ferroan) nontronite in air or argon. (B) Ferric nontronite in H_2/N_2. (C) Ferroan nontronite in H_2/N_2.

from the tetrahedral to the octahedral layer. Certainly, charge imbalance due to reduction will be considerable, and resulting ionic rearrangements involving aluminium should tend to favour the octahedral coordination of this ion, which has an octahedral site preference energy of -42 kJ mol^{-1} (ref. 29).

CONCLUSIONS

The thermal reactions of ferric and ferroan nontronites in air, argon and hydrogen/nitrogen can be represented as follows (the interlayer cations have been omitted for clarity).

(*a*) *Ferric and ferroan nontronite in air or argon*

$$2[(Si, Al)_8Fe_4^{3+}O_{20}(OH)_4] \rightarrow 2[(Si, Al)_8Fe_4^{3+}O_{22}] + 4H_2O$$

$$\rightarrow \underset{\text{(Fe–Si spinel)}}{Fe_8^{3+}Si_6\square_4O_{24}} + 10SiO_2 \rightarrow \underset{\text{(hematite)*}}{4Fe_2O_3} + \underset{\text{(cristobalite)*}}{6SiO_2} \quad (2)$$

(*b*) *Ferric nontronite in hydrogen/nitrogen*

$$2[(Si, Al)_8Fe_4^{3+}O_{20}(OH)_4] \rightarrow 2[(Si, Al)_8Fe_4^{3+}O_{22}] + 4H_2O$$

$$\rightarrow \underset{\text{(fayalite)}}{4Fe_2SiO_4} + \underset{\text{(quartz)}}{12SiO_2} + 4H_2O \rightarrow 6Fe + \underset{\text{(wustite)}}{2FeO} + 4SiO_2 + 6H_2O \quad (3)$$

(*c*) *Ferroan nontronite in hydrogen/nitrogen*

$$2[(Si, Al, Fe^{3+})_8(Fe^{3+}, Fe^{2+}, Mg)_4O_{20}(OH)_4] \rightarrow$$

$$2[(Si, Al, Fe^{3+})_8(Fe^{3+}, Fe^{2+}, Mg)_4O_{22}] + 4H_2O$$

$$\rightarrow \underset{\text{(ferrosilite)}}{8FeSiO_3} + \underset{\text{(magnetite)}}{2/3Fe_3O_4} + 6SiO_2 + 3\tfrac{1}{3}H_2O$$

$$\rightarrow 8Fe + \underset{\text{(quartz)}}{8SiO_2} + \underset{\text{(wustite)}}{2FeO} + 8\tfrac{2}{3}H_2O \quad (4)$$

X-ray diffraction, Mössbauer and IR spectroscopy all suggest that the transformations occur in a continuous sequence of phases dictated by the distribution and valence state of the atoms at each stage of the heating. The loss of interlayer water is concomitant with loss of hydroxyl water, but though these processes give rise to distortion, especially in the octahedral layers, significant reduction or oxidation occurs only towards the completion of dehydroxylation. The thermal reactions can be formulated in terms of an inhomogeneous reaction mechanism, but apart from the observed structural continuity of the phases, no other evidence for such a mechanism is available. The persistence of a maghemite-type spinel phase to temperatures at

*The products of ferroan nontronite include magnetite and tridymite.

which it is normally unstable suggests that it may contain silicon, thereby providing further support for an inhomogeneous mechanism.

ACKNOWLEDGEMENTS

We are indebted to Dr. J. H. Sharp, Sheffield University, for providing the ferroan nontronite, and to Dr. J. W. Waters, N.Z. Geological Survey, for the ferric nontronite. The chemical analyses were by Dr. R. Goguel and Mr. J. Ritchie. Dr. L. P. Aldridge provided the Mössbauer programme and assisted with the computing.

REFERENCES

1 W. E. Addison and J. H. Sharp, *Clays Clay Miner.*, 11 (1963) 95.
2 G. M. Bancroft, A. G. Maddock and R. G. Burns, *Geochim. Cosmochim. Acta*, 31 (1967) 2219.
3 J. L. Bischoff, *Clays Clay Miner.*, 20 (1972) 217.
4 T. Sudo and T. Nakamura, *Am. Miner.*, 37 (1952) 618.
5 R. E. Grim and G. Kulbicki, *Am. Miner.*, 46 (1961) 1329.
6 W. F. Bradley and R. E. Grim, *Am. Miner.*, 36 (1951) 182.
7 C. E. Weaver, J. M. Wampler and T. E. Pecuil, *Science*, 156 (1967) 504.
8 G. L. Taylor, A. P. Ruotsala and R. O. Keeling, *Clays Clay Miner.*, 16 (1968) 381.
9 C. S. Ross and S. B. Hendricks, *U.S. Geol. Surv. Prof. Pap.*, 205-B (1945).
10 P. E. Clark, A. W. Nicol and J. S. Carlow, *J. Sci. Inst.*, 44 (1967) 1001.
11 A. J. Stone ,H. J. Aagaard and J. Fenger, *Dan. A. E. C., Risoe Rep.*, RISO-M 1348, (1971).
12 N. H. Brett, K. J. D. MacKenzie and J. H. Sharp, *Q. Rev.*, 24 (1970) 185.
13 F. D. Richardson and J. H. E. Jeffes, *J. Iron Steel Inst.*, 160 (1948) 261.
14 M. W. Molloy and P. F. Kerr, *Am. Miner.*, 46 (1961) 583.
15 D. H. Lindsley, B. T. C. Davis and I. D. Macgregor, *Science*, 144 (1964) 73.
16 O. E. Floerke, *Naturwissenschaften*, 43 (1956) 419.
17 V. C. Farmer and J. D. Russell, *Spectrochim. Acta*, 20 (1964) 1149.
18 D. A. Duke and J. D. Stephens, *Am. Mineral.*, 49 (1964) 1388.
19 E. R. Lippincott, A. Van Valkenburg, C. E. Weir and E. N. Bunting, *J. Res. Nat. Bur. Stand.*, 61 (1958) 61.
20 R. M. Golding, *Applied Wave Mechanics*, Van Nostrand, London, 1969, p. 424.
21 N. N. Greenwood and T. C. Gibb, *Mössbauer Spectroscopy*, Chapman and Hall, London, 1971, p. 247.
22 W. R. Bush, S. S. Hafner and D. Virgo, *Nature, London*, 227 (1970) 1339.
23 E. K. Dowty and D. H. Lindsley, *Am. Mineral.*, 58 (1973) 850.
24 R. Steadman and R. F. Youell, *Nature, London*, 180 (1957) 1066.
25 G. W. Brindley, *Prog. Ceram. Sci.*, 3 (1963) 3.
26 G. W. Brindley and M. Nakahira, *J. Am. Ceram. Soc.*, 42 (1959) 311.
27 K. J. D. MacKenzie, *Trans. J. Br. Ceram. Soc.*, 72 (1973) 209.
28 R. E. Grim, *Clay Mineralogy*, McGraw-Hill, NY, 1953 p. 226.
29 A. Navrotsky and O. J. Kleppa, *J. Inorg. Nucl. Chem.*, 29 (1967) 2701.